Article

Smoke toxicity of rainscreen façades

Peck, Gabrielle, Jones, Nicola, Mckenna, Sean Thomas, Glockling, Jim L D, Harbottle, John, Stec, Anna A and Hull, T Richard

Peck, Gabrielle, Jones, Nicola ORCID: 0000-0002-1985-5266, Mckenna, Sean Thomas, Glockling, Jim L D, Harbottle, John, Stec, Anna A ORCID: 0000-0002-6861-0468 and Hull, T Richard ORCID: 0000-0002-7970-4208 (2020) Smoke toxicity of rainscreen façades. Journal of Hazardous Materials, 403 . p. 123694. ISSN 0304-3894

Citation: Peck, G., Jones, N., McKenna, S.T., Glockling, J.L.D., Harbottle, J., Stec, A.A., Hull, T.R.
Smoke toxicity of rainscreen façades, (2021) Journal of Hazardous Materials, 403, art. no. 123694,
https://doi.org/10.1016/j.jhazmat.2020.123694

Smoke toxicity of rainscreen façades

Gabrielle Peck[1], Nicola Jones[1], Sean T McKenna[1], Jim L. D. Glockling[2], John Harbottle[2], Anna A. Stec[1], and T. Richard Hull[1]*.

1. Centre for Fire and Hazard Science, University of Central Lancashire, Preston, PR1 2HE, UK
2. Fire Protection Association, London Road, Moreton in Marsh, Gloucestershire, GL56 0RH, UK

* corresponding author trhull@uclan.ac.uk

Abstract

The toxic smoke production of four rainscreen façade systems were compared during large-scale fire performance testing on a reduced height BS 8414 test wall. Systems comprising 'non-combustible' aluminium composite material (ACM) with polyisocyanurate (PIR), phenolic foam (PF) and stone wool (SW) insulation, and polyethylene-filled ACM with PIR insulation were tested. Smoke toxicity was measured by sampling gases at two points - the exhaust duct of the main test room and an additional 'kitchen vent', which connects the rainscreen cavity to an occupied area. Although the toxicity of the smoke was similar for the three insulation products with non-combustible ACM, the toxicity of the smoke flowing from the burning cavity through the kitchen vent was greater by factors of 40 and 17 for PIR and PF insulation respectively, when compared to SW. Occupants sheltering in a room connected to the vent are predicted to collapse, and then inhale a lethal concentration of asphyxiant gases. This is the first report quantifying fire conditions within the cavity and assessing smoke toxicity within a rainscreen façade cavity.

Keywords: Incapacitation; lethality; carbon monoxide; CO; hydrogen cyanide; HCN; polyisocyanurate; PIR; phenolic; stone wool; fire; combustion.

1 Introduction

Rainscreen facades are increasingly popular for new and refurbished buildings, usually consisting of a thin outer panel (4-12 mm), a ventilated cavity (50 mm) and a layer of insulation (60-200 mm). Aluminium composite material (ACM) panel products range from polyethylene-filled aluminium composite material (ACM-PE) to non-combustible metal or mineral wool panels. In each case, the panels are made with architecturally interesting paint coatings, giving a modern look to a new or refurbished building.

Ventilated cavities prevent moisture build-up in building façades. However, in the event of a fire, the cavity behaves as a chimney with its combustible walls supporting rapid fire and smoke spread[1,2]. Cavity barriers are required to be installed at specific locations as part of a ventilated facade to prevent fire spread, although they are sometimes incorrectly installed or are missing altogether.

In 2016, Grenfell Tower underwent refurbishment, including the addition a rainscreen façade to improve the thermal insulation and appearance of the building. A combination of polyisocyanurate (PIR) and phenolic foam (PF) insulation was attached to the external walls of the building and faced with ACM-PE with a 50 mm cavity in between. All three façade products were combustible but arguably compliant with the building regulations in force at the time, based on desktop studies[3] showing they would be likely to meet the BR 135 criteria in a BS 8414 test[4]. A critique of the BS 8414

standard, the BR 135 criteria, and the DCLG tests has been reported elsewhere[5]. Three combustible insulation products were reported to have met these criteria, two phenolic foams and one PIR foam. In June 2017, the façade system fuelled the fire that began on the fourth floor of the building and spread rapidly. Within minutes, the fire had spread across the external façade of the building ultimately taking the lives of 72 people[6]. Inhalation of toxic smoke is the greatest cause of fatality in unwanted fires, and the greatest source of injury[7]. During the flaming combustion of PIR, hydrogen cyanide is produced in significant quantities[8,9]. Other toxicants such as isocyanates are also produced[10, 11]. Several Grenfell survivors were treated for cyanide poisoning[12].

The danger of combustible façade systems has been a recurring problem. Previous cladding fires include the 1991 Knowsley Heights fire and the 1999 Garnock Court fire[13]. In 2009, a fire spread from a balcony at Lakanal House, a tower block in London. The fire spread through the high-pressure laminate panelling that had been added during a prior refurbishment, resulting in the deaths of six people. Five of the deaths were confirmed to be a result of smoke inhalation, while the victims were sheltering in a bathroom, with fumes reaching them from a vent linked to the cavity[14].

Following the Grenfell Tower disaster, the Department for Communities and Local Government (DCLG but now the Ministry of Housing and Local Government (MHCLG)) commissioned a series of seven initial large scale tests using BS 8414[15] on three types of ACM panels, combined with PIR, phenolic foam and stone wool insulation[16]. An eighth test, on fire retarded HPL panels with stone wool insulation was also undertaken in July 2019[17]. Despite the importance of smoke inhalation to fire deaths[7,12], smoke toxicity was not measured in any of the DCLG tests.

In small, well-ventilated flaming conditions, materials burn completely to carbon dioxide, water and nitrogen gas (if N is present in the fuel). As the fire grows, the rate of burning is limited by the availability of oxygen, and again more products of incomplete combustion, such as CO and HCN are produced[18]. The smoke toxicity of insulation products has been reported elsewhere[8]. Alternative non-combustible products, such as mineral wools and more recently aerogels[19], are able to provide thermal insulation without these hazards. The danger of smoke toxicity, and the release of HCN from rigid and flexible urethane foams is well-established[20]. It has been shown that when PIR foam burns it generates HCN and CO in dangerous quantities[9]. PIR foam was originally developed to make use of waste isocyanates, used in polyurethane foam (PUR) manufacture[21]. The excess isocyanate formed isocyanurate trimers with excellent thermal stability, giving PIR foam lower flammability than PUR foam. As PIR popularity increased, so the availability of waste isocyanate diminished: modern PIRs have under half the isocyanate content of the original, and require significant quantities of trichloro alkyl phosphate (TCAP) flame retardants to meet flammability criteria. The presence of gas-phase flame quenchers, such as halogenated flame retardants, interferes with this process, increasing the yield of carbon monoxide (CO), and when nitrogen is present hydrogen cyanide (HCN)[22] . The TCAP family of flame retardants have also come under increasing scrutiny due to their intrinsic toxicity[23] , presence in the aquatic environment[24] and household dust[25]. Attempts to reduce the smoke toxicity of polyurethanes have been reported[26], but many focus on thermoplastic polyurethanes[27,28] or relate to non-flaming decomposition conditions[29].

The fire properties of a range of rainscreen panels and insulation, suitable for use on buildings of over 18 m, have been reported elsewhere[30]. The experimental part of the current work was conducted in 2018 before the UK government announced a ban on all combustible materials (performance must now be Euroclass A2 s1 d0 or better) on the external walls of new or refurbished residential buildings over 18 m. The ban does not include hotels, offices, hospitals or buildings below 18 m, and is not retrospective. A summary of this work was reported before the combustibles ban, in 2018[31].

A series of four façade systems were constructed using a reduced height BS 8414-1 test wall (5 m) with the aim of quantifying the toxicity of the smoke by sampling at two locations. This allowed comparison of the fire effluent toxicity produced by each façade system. In addition to monitoring the smoke toxicity in the main exhaust duct of the test chamber, a kitchen vent, typical of one installed between a kitchen or bathroom and the façade of a tower block, was incorporated into the facade system. The vent provided a direct route for the smoke to travel from the cavity to a hypothetical room in an apartment, so that the toxicity of the gases within the cavity could be quantified. In a real building, this toxic smoke may also enter the apartment through open or broken windows or voids within the structure.

The precise details of the materials and manner of construction also affects the fire behaviour of a façade. The test façades in this work followed normal industry practice: typical designs, construction materials and installation practice were used. The importance of including additional fixings and openings to building façades during large scale façade testing has been highlighted[32, 33] and there is presently a knowledge-gap in this area.

1.1 Quantification of fire effluent toxicity

Quantification of fire effluent composition enables prediction of both incapacitation (inability to escape unaided) and lethality (based on rat lethality data) using ISO 13571[34] and ISO 13344[35] respectively.

Toxic effects of fire effluent can be expressed as a Fractional Effective Dose (FED), based on the chemical composition of the effluent. When the FED is equal to one, 50% of a healthy, adult exposed population would be predicted to suffer incapacitation or death. In both cases carbon dioxide (CO_2) increases respiration rate and so a multiplication factor for CO_2-driven hyperventilation, V_{CO_2} is included in the calculation (Equation [3]). ISO 13571[34] stipulates the use of Equation [1] for estimation of incapacitation by the asphyxiant gases carbon monoxide (CO) and hydrogen cyanide (HCN):

$$FED = \left\{\sum_{t_1}^{t_2} \frac{[CO]}{35000}\Delta t + \sum_{t_1}^{t_2} \frac{[HCN]^{2.36}}{1.2\times10^6}\Delta t\right\} \times V_{CO_2} \quad [1]$$

Gas concentrations in [] are expressed in μL L^{-1} or ppm; time (*t*) is in minutes.

Equation [2], from ISO 13344[35] provides an estimation of lethality for a 30-minute exposure, using the ratio of each toxicant concentration to its lethal concentration (LC_{50}). Carbon dioxide (CO_2) increases respiration rate and so a multiplication factor for CO_2-driven hyperventilation, V_{CO_2} is included in the calculation. An acidosis factor, A, is included to account for CO_2 toxicity via acidosis. AGI are acid gas irritants and OI are organic irritants.

$$FED = \left\{\frac{[CO]}{LC_{50,CO}} + \frac{[HCN]}{LC_{50,HCN}} + \frac{[AGI]}{LC_{50,AGI}} + \frac{[OI]}{LC_{50,OI}} \ldots\right\} \times V_{CO_2} + A + \frac{21-[O_2]}{21-5.4} \quad [2]$$

$$V_{CO_2} = 1 + \frac{\exp(0.14[CO_2])-1}{2} \quad [3]$$

The acidosis factor A = $[CO_2]$ x 0.05. O_2 and CO_2 concentrations are expressed in vol %. The concentration of the other toxicants is in μL L^{-1} or ppm.

it is important to recognise that hazard prediction describes an unacceptable outcome of incapacitation or lethality. In any hazard or risk assessment, a factor of 0.3 is applied for a healthy adult population to ensure that around 90% of the trapped fire victims do not suffer the outcomes above, and another factor of 0.3 is applied to that figure if typical human populations, such as office

workers, are considered, in order to account for individuals of greater susceptibility. Thus, a value of FED = 0.1 for effluent flowing into an apartment would be considered an unacceptable hazard.

2 Experimental

2.1 Materials

Four combinations of insulation and facade panels typical of rainscreen cladding systems, used on buildings larger than two-storey houses throughout the UK, were tested in the reduced height BS 8414 test facility, as shown in Table 1.

Table 1. Combinations of insulation and facade panels.

Abbreviation	Insulation	Facade panel
SW/A2	Stone wool	ACM-A2 (mineral core)
PF/A2	Phenolic foam	ACM-A2 (mineral core)
PIR/A2	Polyisocyanurate foam	ACM-A2 (mineral core)
PIR/PE	Polyisocyanurate foam	ACM-PE (polyethylene core)

ACM consists of two, 0.5 mm thick, aluminium sheets, with a 3 mm thick core of either: mineral material with less than 5% organic binder[30] (ACM-A2), Fire retarded PE (ACM-FR) or PE (ACM-PE).

For the plastic foams, the insulation thickness was 100 mm, for the stone wool it was 180 mm in order to compare similar insulation capacities. The cavity was protected by mineral wool and intumescent strip cavity barriers in accordance with Approved Document B[36].

SW/A2 was used as a control, since both the insulation and the ACM panel were of limited combustibility (Euroclass A2 or above). The PF/A2 and PIR/A2 combinations represent a limited combustibility ACM panel being used to protect the underlying combustible foam insulation. PIR/PE consists of combustible ACM *and* combustible insulation and is the combination that was most widely found on Grenfell Tower. The DCLG test, using BS 8414-1, on this combination was stopped after around 8 ½ min after ignition.

PIR/PE, the combination of PIR insulation with ACM-PE, represents the system used in most of the facade on Grenfell Tower. The phenolic foam, reported to have met the BR135 criteria, was still available at the time of testing. The PIR used was a chemically similar substitution from the same manufacturer, as the original product had been withdrawn after the Grenfell Tower fire.

2.2 Experimental construction

Tests were carried out in a corrugated steel and masonry building, measuring 10 m x 10 m x 6 m high. During each test, the roller shutter to the test building, measuring 2 m wide, was left open to a height of 1 m to provide a supply of fresh air. The ceiling of the room contained a 2.5 m x 2.5 m grille linked to an extraction system, pumped at approximately 1.5 m^3 s^{-1} with flow measured using McCaffrey (bi-directional) probes.

The tests were conducted using the structure defined in BS 8414-1[15] with a reduced height of 5 m rather than the standard 8-9 m. The L-shaped test wall was a standard-construction masonry block wall. The façade design was based on designs for actual building projects. Installation of each façade system was by commercial façade installers and followed normal building practice with the inclusion of cavity barriers at specific locations. Each façade was fixed directly to the wall by brackets and included a 50 mm cavity between the insulation and the 4 mm thick rainscreen panel.

A 'kitchen vent' was included in the installation, which consisted of a 100 mm diameter circular galvanised steel pipe, which was open to the cavity and faced with a 150 mm x 150 mm steel grille mounted on the ACM panel. Figure 1 shows a diagram and photograph of the test wall, with an inset showing an enlarged photograph of the vent.

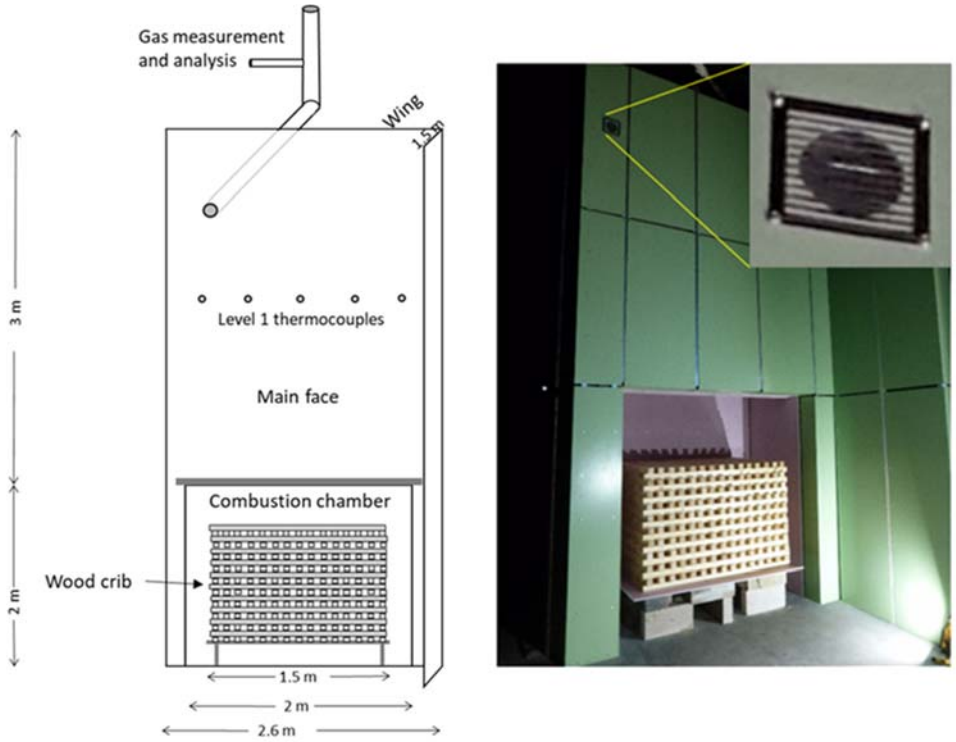

Figure 1 Diagram of the test wall configuration and photograph of test set up. Inset shows the external face of the kitchen vent

2.3 Gas sampling

Tests were carried out for 1 hour. Gas sampling was stopped after 30 minutes (before extinguishment with a water jet) to prevent water condensate entering the gas analysers.

Custom-built sampling boxes containing NDIR (Non-dispersive Infra-red) analysers and mass flow controllers were used for continuous monitoring of carbon monoxide (CO), carbon dioxide (CO_2) and oxygen (O_2). Hydrogen cyanide (HCN) was quantified by bubbling metered volumes of fire effluent through aqueous sodium hydroxide solution (0.1 mol dm^{-3}) at five-minute intervals throughout the test, and analysed colorimetrically following the method in ISO 19701[37]. Dreschel bottles containing de-ionised water were used to trap acid gases, for analysis by high performance ion-chromatography (HPIC).

Sampling lines for gas analysis, and probes to measure the velocity and temperature of the gases, were installed at two points.

2.3.1 Main Test Room Exhaust

Sampling at this point was used to gather baseline toxicity data, since the majority of smoke entering the extraction system was produced by the burning wood crib and was similar for each test.

2.3.2 Kitchen Vent

The position of the vent within the test facility, including the position of the sampling point can be seen in Figure 2. The horizontal vent duct was installed through the masonry wall of the test rig and

exited the corrugated steel structure (2 m) before rising vertically (1 m) outside the test facility. This allowed a natural flow through the duct. It is acknowledged that in a real fire the flow is likely to be driven by more than buoyancy alone, and will differ significantly from that found here, dependant on factors including wind, fire development and ventilation from within the structure.

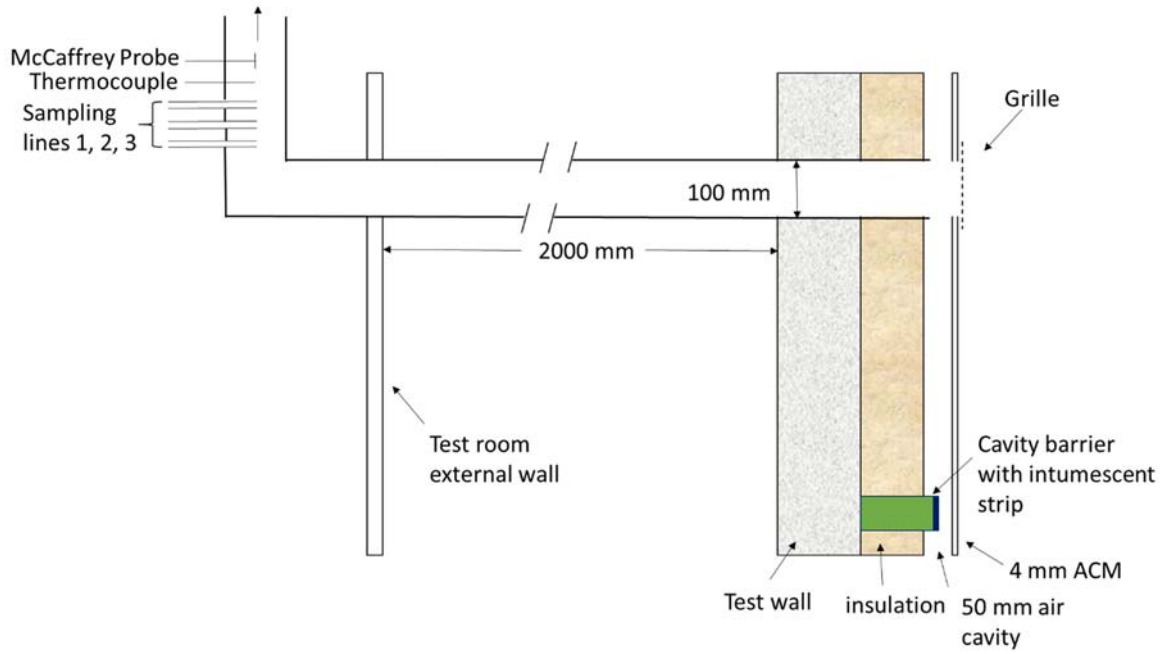

Figure 2 Cross-section of the test wall

Three sampling lines, a thermocouple and a McCaffrey probe were installed in the vertical section of the duct to measure gaseous effluents travelling through the vent.

3 Results and Discussion

3.1 Sampling times

Each test ran for 60 min from ignition; wood cribs were extinguished after 30 min in all tests except the PIR/PE test, which was extinguished after 13.5 min due to structural safety concerns for the test building. During the PIR/A2 test, a sampling line from the kitchen vent touched the hot surface of the vent and melted, 27 min into the test, preventing further gas sampling by NDIR.

3.2 ACM panel integrity

During the tests it was apparent that the ACM-A2 panels did not adequately protect the insulation from fire. The central front panels were seen falling from the test wall as the panels and their aluminium support rails lost their structural integrity on exposure to the fire. As a result, the insulation was exposed to the fire. For SW/A2 the exposed insulation remained attached to the wall for the remainder of the test. For PF/A2 and PIR/A2 the exposed insulation began to burn and eventually fell from the wall. In Figure 3 enlarged photographs of the test walls after the end of the test show how the ACM failed and how much the insulation and particularly the façade section around the kitchen vent became involved. The PIR/PE test showed very rapid fire growth, apparent showers of burning droplets, and copious quantities of black smoke. Little, if any of the ACM-PE remained in place. The photograph (Figure 3d) shows the extent of loss of the ACM-PE and PIR panels in the first 13.5 min, in contrast with the A2 façades, which were allowed to burn for the full 60 min. Despite extinguishment, the PIR char had flared up again when the photograph was taken.

Figure 3 Remains of the tests showing damage around the vent. a) SW/A2, b) PF/A2, c) PIR/A2, d) PIR/PE

3.3 Cavity breakthrough times

The concentrations of O_2, CO_2 and CO were recorded at the kitchen vent alongside those at the main exhaust, used as baseline data. The point at which the vent concentrations for each façade combination deviated from the baseline is very clear. At these points the vent O_2 concentration decreased sharply, with a corresponding sharp increase in CO_2 and CO concentrations. These deviation points correspond to the time when the fire broke through to the part of the cavity containing the kitchen vent, as the ACM became detached, allowing direct access of the fire to the insulation in that section. For PIR/PE this took 7 minutes, for PIR/A2 it took 22 minutes and for PF/A2 it started at around 21 minutes where an initial change is seen, then after 28 minutes a further, sharper change is seen. SW/A2 appears to have broken through at 17 minutes, but since only a decrease in O2 was seen, and there was no increase in CO or CO2 concentration. It is difficult to explain the cause of the oxygen depletion in the cavity.

3.4 Gas concentrations

3.4.1 Oxygen, carbon dioxide and carbon monoxide concentrations

Figure 4 shows both the baseline and kitchen vent O_2 data for all tests. The O_2 concentrations clearly show the point at which the fire broke through into the vent section of the cavity. For SW/A2, the O_2 concentration decreased to 7%. For PF/A2 and PIR/A2 the O_2 concentration decreased steadily to the point of breakthrough, where it then decreased sharply to around 1% in both cases. The initial steady decrease is likely to result from fire effluent from the burning wood crib flowing into the cavity, and the sharp decrease is due to pyrolysis of the PIR or PF foam behind the rainscreen panels (an effect which is much reduced for stone wool insulation due to its low organic content (~ 5%)[30]. For PIR/PE the O_2 concentration decreased much earlier (7 min) than for the other tests and was 4% when the test was stopped after 13.5 min.

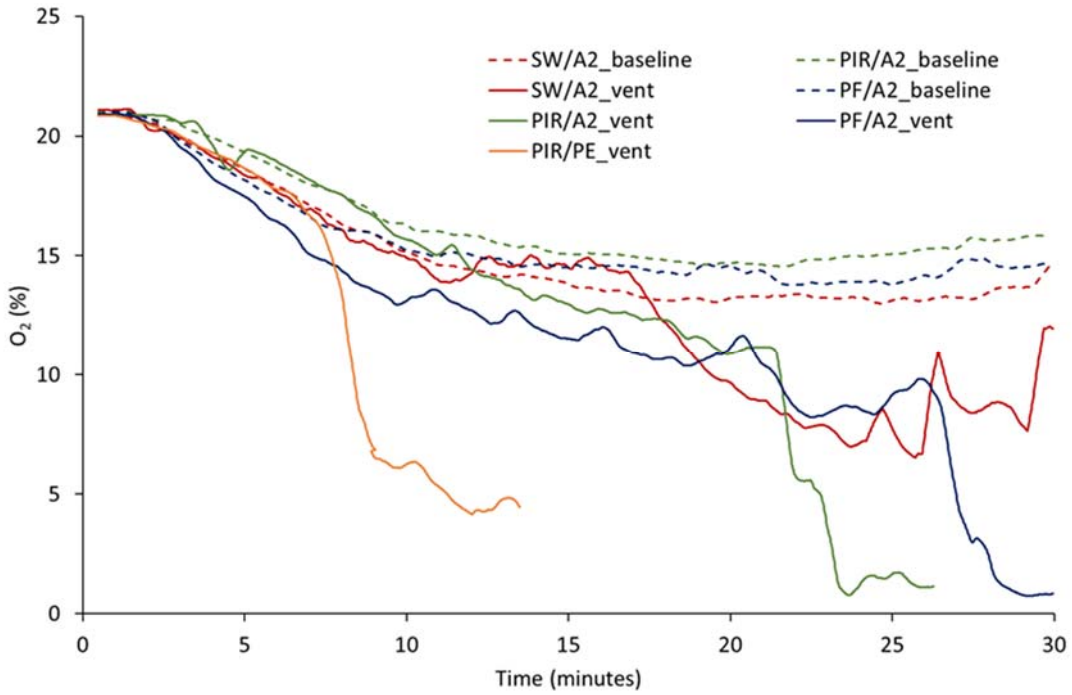

Figure 4 O_2 baseline and vent concentrations

Figure 5 shows the CO_2 baseline and the kitchen vent concentration data. For SW/A2, the CO_2 concentration at the vent did not deviate significantly from the baseline. For PIR/A2 and PF/A2, the CO_2 concentrations progressively increased until the fire breakthrough point, when a sharp increase occurred, rising to around 18 %.

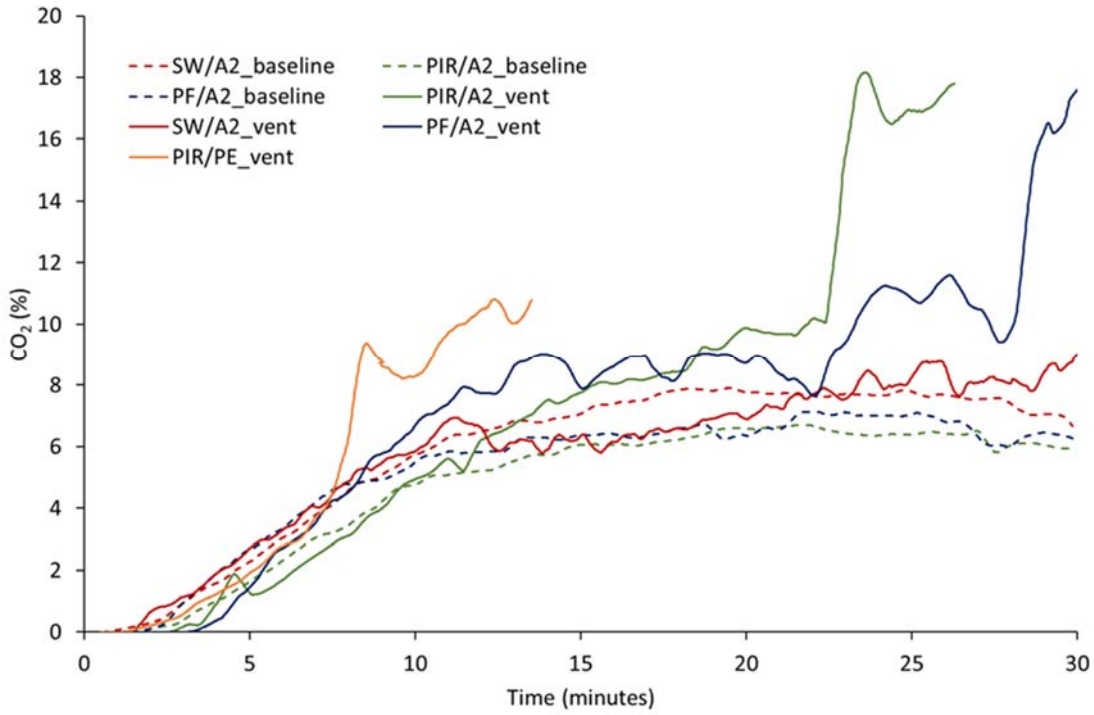

Figure 5 CO_2 baseline and vent concentrations

Figure 6 shows the CO baseline and kitchen vent concentrations. The chart shows that for SW/A2, the CO concentration did not deviate significantly from the baseline. The CO concentrations for PF/A2 and PIR/A2 increased very sharply at the point of breakthrough, reaching very high concentrations. This was likely due to the insulation burning behind the panel, below the kitchen vent aperture, in under-ventilated conditions. Again, the CO concentration increased much earlier for PIR/PE than for the other combinations. Yields of CO have been shown to increase from burning polymers, both with the use of flame retardants acting in the gas-phase[22] and with under-ventilation[18,38].

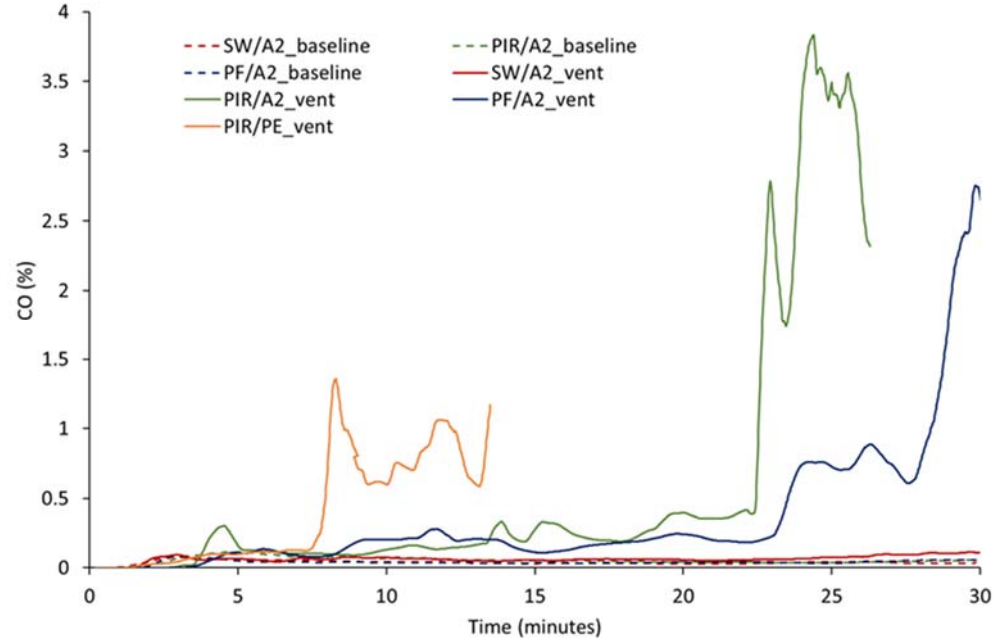

Figure 6 CO baseline and vent concentrations

3.4.2 Hydrogen cyanide concentration

Figure 7 shows the baseline and vent concentrations of HCN. As HCN was collected in bubblers at 5 min intervals, less temporal variation is available. The baseline data for all tests was around 15 ppm. The chart shows that for SW/A2, the HCN concentration did not deviate significantly from the baseline level. For PF/A2, the HCN increased to a concentration of around 250 ppm, and for PIR/A2 it increased to around 500 ppm. PIR contains around 8% nitrogen by mass[30] and yields significant quantities of HCN during flaming combustion, increasing with under-ventilation[39]. Urea is added to phenolic foam during production to increase cross-linking, so it contains around 2% nitrogen by mass[30], facilitating the production of HCN. For the PIR/PE combination, the HCN concentration increased earlier than for the other tests, increasing to 60 ppm just before the test was stopped, after 13.5 min. The increase in HCN yields measured after 20 minutes for PIR/A2 and PF/A2 are due to increased under-ventilated flaming in the cavity, and the use of gas phase flame retardants.

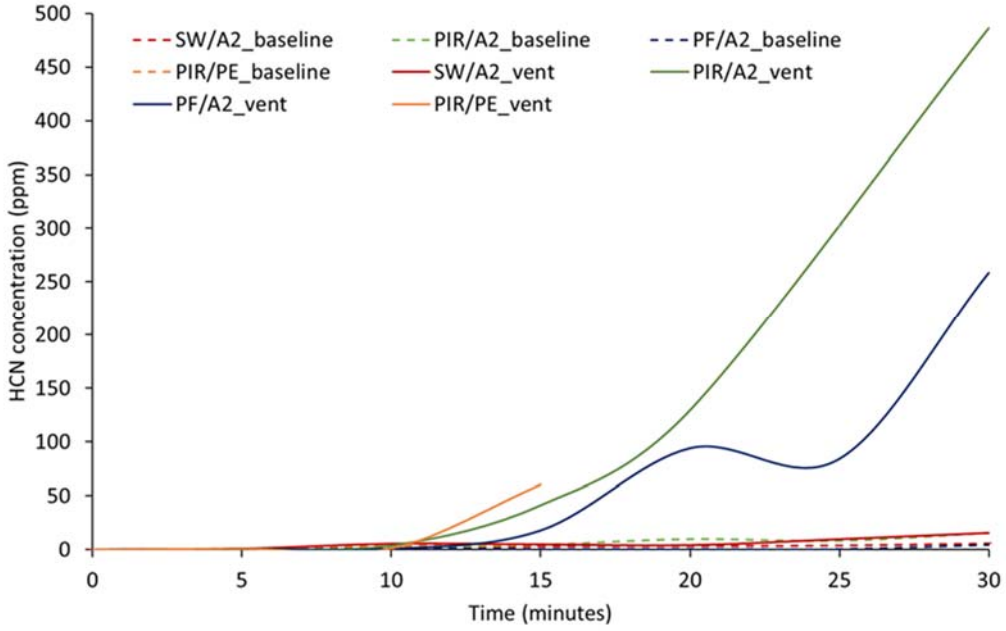

Figure 7 HCN baseline and vent concentrations

In order to explain why the CO and HCN concentrations in the vent were so high, it is necessary to understand the fire conditions in the ventilated cavity.

3.5 Fire conditions within the façade cavity

The oxygen concentrations (Figure 5), and the CO/CO_2 ratio, can be used to identify the fire stage within the façade according to the characteristic stages of flaming combustion, given in ISO 19706[40] and summarised in Table 2.

Table 2 Characteristics of fire stage[40]

Fire Stage	Condition	Oxygen Vol. %		$[CO]/[CO_2]$
		Entrained	Exhausted	v/v
2	Well-ventilated	~20	~20	<0.05
3 a	Small, under-ventilated	15 to 20	5 to 10	0.2 to 0.4
3 b	Large, under-ventilated	<15	<5	0.1 to 0.4

The entrained oxygen % entering the façade will equal the baseline oxygen concentration, while the exhausted oxygen % will equal the vent oxygen concentration. This indicates a shift to under-ventilated flaming within the façade for PIR/PE, PIR/A2, and PF/A2, and possibly even SW/A2. Figure 8 shows the CO/CO_2 ratios of the gases measured within the kitchen vent throughout each test. The initial peak in Figure 8, before 5 min, is a result of the ignition of the crib (CO is also a significant product of oxidative pyrolysis, before the wood has fully ignited). Behind the cavity, after 5 min, the CO/CO_2 ratio was characteristic of well-ventilated flaming until the fire was able to access the combustible insulation. For SW/A2 the CO/CO_2 ratio was characteristic of well-ventilated flaming throughout the test.

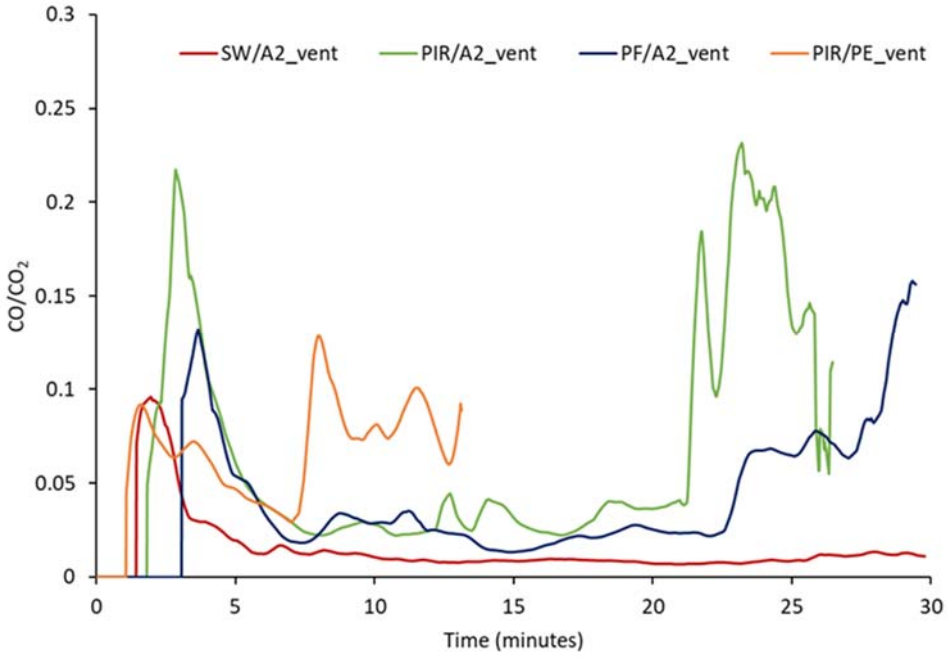

Figure 8 CO/CO_2 ratios

At the point of fire break-through into the cavity the CO/CO_2 ratio became greater than 0.1 as the insulation started to burn, creating under-ventilated flaming conditions within the cavity. For PIR/A2, flaming within the vent section of the cavity became under-ventilated after around 21 min; for PF/A2 it was around 28 min; for PIR/PE the under-ventilated condition was not sustained, possibly because the burning PE destroyed the ACM and opened-up the cavity.

3.6 Smoke Toxicity

The toxicity of the fire effluent measured in the kitchen vent was calculated and expressed as FEDs in order to predict incapacitation and lethality in the hypothetical 30 m3 room for the four façade systems tested. Since, in these tests, the kitchen vent was not pumped, there was no significant flow of toxicants through it until the point of breakthrough. After this, the smoke flowed quickly which would result in rapid accumulation of toxic gases. This provides a snapshot of the potential toxicity,

which could be much higher, or lower, in a real apartment depending on wind and smoke flow. In addition, during these tests the analysers were stopped very soon after breakthrough. The toxicity has been predicted using the concentrations and flow of fire effluents measured in the kitchen vent. The flow rates of the effluents through the kitchen vent are shown in Figure 9 below.

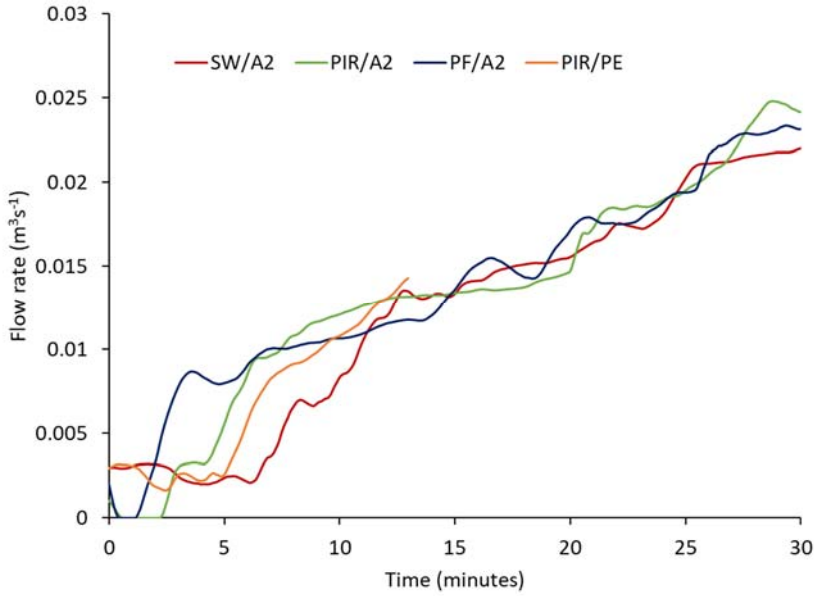

Figure 9 Flow rates of fire effluents through the kitchen vent

The FED data were calculated based on the fire effluent flowing through the kitchen vent into an empty, hypothetical room of volume 30 m^3, which could have dimensions of 3.4 m x 3.4 m x 2.6 m high. The calculation assumes that the gases had mixed completely. If a hotter upper layer existed, 30 m^3 of toxic smoke could have filled the upper 1.5 m layer of a larger 2.5 m high room of dimensions 4.3 m x 4.3 m. FED data for PIR/A2 has been provided as an extrapolation after 27 minutes. For the purpose of calculation, it has been assumed that the small volume flowing into the room during the test (up to ~0.025 m^3 s^{-1}) only displaces fresh air in the room.

The predicted toxicity of the fire effluent flowing into the 30 m^3 room via the kitchen vent has been expressed as FEDs for incapacitation and lethality for the three ACM-A2 façade systems, shown in Table 3. This shows the danger to occupants from façade vents, open or broken windows etc. The equations predict incapacitation or lethality of 50% of the exposed population when FED = 1.

Table 3 Calculated FEDs for incapacitation and lethality at the kitchen vent 30 min after ignition.

FED	SW/A2	PIR/A2	PF/A2
Incapacitation	0.04	1.56	0.64
Lethality	0.80	3.78	2.18

3.6.1 Incapacitation

Figure 10 shows how the FED for incapacitation by asphyxiants increases during each test based on a 30 m3 room filling with smoke from the kitchen vent. When the FED equals 1 then incapacitation is predicted for 50 % of the population exposed to the fire effluent. No useful predictions can be made

for FED values above or below 1, except that the exposure volume could be increased or decreased until the FED = 1.

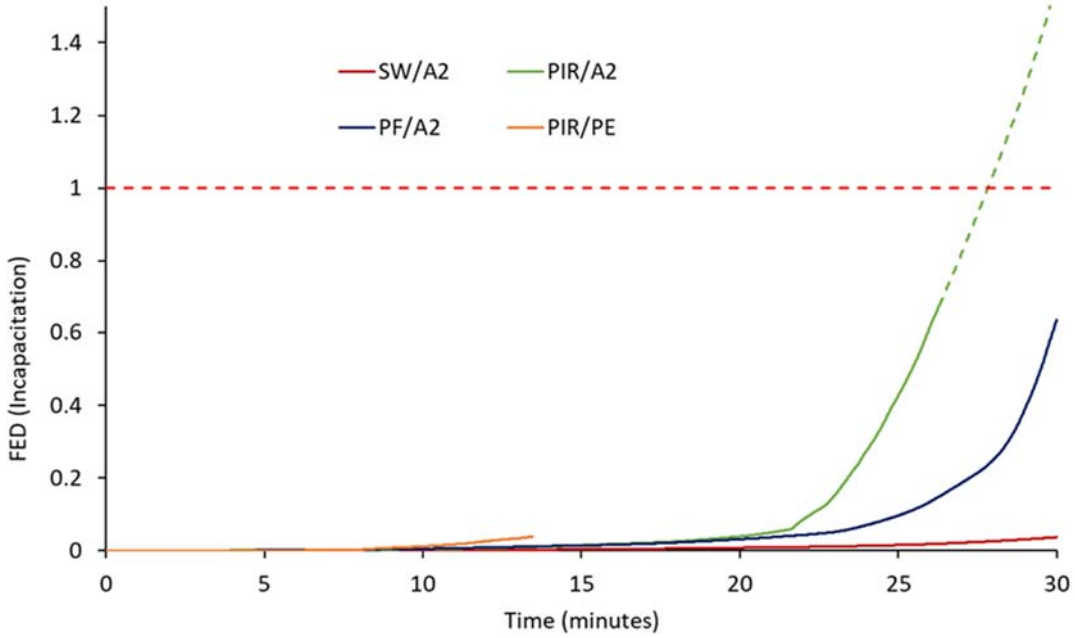

Figure 10 Cumulative FED (incapacitation)

Since the FED for SW/A2 was less than 0.05 after the 30-minute test, the time to incapacitation cannot be predicted, but given that the fire broke through into the vent section at around 17 min, it seems unlikely that incapacitation would occur within 60 min of ignition with this material combination. For PF/A2 the FED reached 0.6, and the trend suggests that incapacitation would have occurred around 32 min, or about 5 min after breakthrough.

For PIR/A2, a sharp increase in the FED occurred after the point of fire breakthrough (22 min), and incapacitation is predicted within about 5 min, at 27 min. At that point half of the exposed population would probably lose consciousness and be unable to effect their own escape. The sharp increase of the curve suggests the remainder of the exposed population would suffer the same fate very soon afterwards.

For PIR/PE, the FED starts to increase much earlier than the other tests, but a full data set was not obtained due to the short test time and the urgent need to extinguish the fire. Figure 10 shows how rapidly untenable conditions develop when combustible insulation is present, once the fire breaks through the barrier into that section of the façade. This can occur if either the cavity barrier fails to form a seal, or if the panel is compromised or destroyed by fire, so there is no surface for the cavity barrier to seal onto. The actual flow of effluent through the kitchen vent will be subject to many factors, including the wind and pressure variations between inside and outside, and may be much greater than the simple buoyant flow reported here.

As the FED calculation is made up of both a CO and an HCN contribution, the data can be separated to identify the relative contributions of each toxicant to incapacitation over the 30 minute test period (Figure 11). It is important to note that for most of this period, the fire had not broken

through to the vent section of the façade. Figure 11 shows that the main contributor to incapacitation is CO for all combinations, for PIR/A2 the total FED of 1 is reached by CO alone. To an extent this is a result of the arbitrary flow rates and size of the hypothetical room. As CO incapacitation is proportional to concentration, but HCN incapacitation is proportional to the HCN concentration raised to the power 2.36 ($[HCN]^{2.36}$), a smaller room would reverse the relative contributions. The contribution of HCN to toxicity from PIR/A2 reflects the greater amount of HCN produced. The total FED for SW/A2 is very low, most probably because although the fire broke through into the cavity the façade materials did not burn.

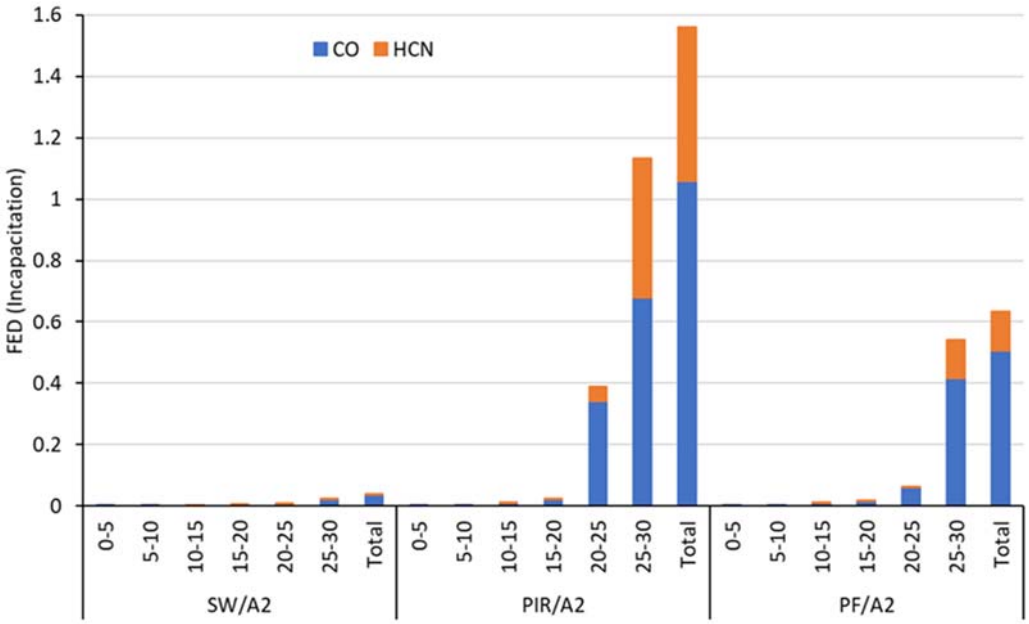

Figure 11 Individual asphyxiant contribution to total FED (incapacitation)

3.6.2 Lethality

Figure 12 shows the FED for lethality over the course of each test, based on a hypothetical 30 m^3 room filling evenly with smoke from the kitchen vent. The FED was calculated based on the same gas concentrations in the hypothetical room, but with an additional 30 min exposure. Therefore, for PIR/A2, incapacitation would occur around 27 min and lethality conditions would have developed after 22 min, so death would be predicted after (22+30 =) 52 min. For PF/A2 incapacitation would occur after 32 minutes and lethality is predicted to occur after (25+30 =) 55 minutes. This is surprising because despite significant differences in the smoke toxicity of these two façade systems, death is predicted very soon after PIR/A2 for PF/A2. This exponential increase in toxic gas concentrations is typical of a rapidly growing fire (or the fire rate dominates the increase in toxicity). Had the same effluent filled an escape route at relatively static toxicant concentrations, the effects of the different materials would be more pronounced. The lethality of the SW/A2 combination is driven by the toxicity of smoke from the burning crib. This could be interpreted as saying that even in a building with a non-combustible façade, toxicity deaths may be expected from burning contents of a fire in an apartment immediately below. However, without flame spread through the façade, only the apartment immediately above would be expected to have a high concentration of toxic gases from the burning contents below.

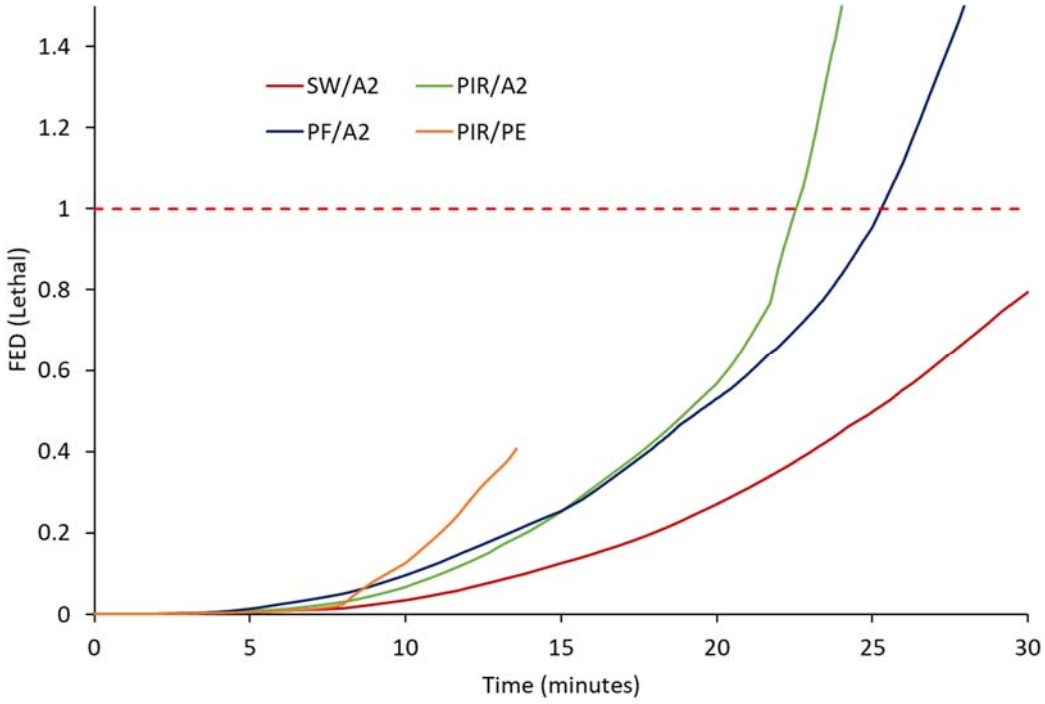

Figure 12 Cumulative lethal FED for 30 minutes exposure

Figure 13 shows the contribution to lethality from all toxicants over the 30-minute test period and the total lethal FED for each 30-minute test. The data include the effect of CO_2 toxicity (acidosis) and oxygen depletion, in addition to CO and HCN concentration as part of the overall FED calculation. The contribution of acidosis and low O_2 were similar for each test. The acidosis and low oxygen (hypoxia) data were fairly typical of the well-ventilated burning of a wood crib for each test, and show how the atmosphere in the test facility and the vent is dominated by smoke from the wood crib.

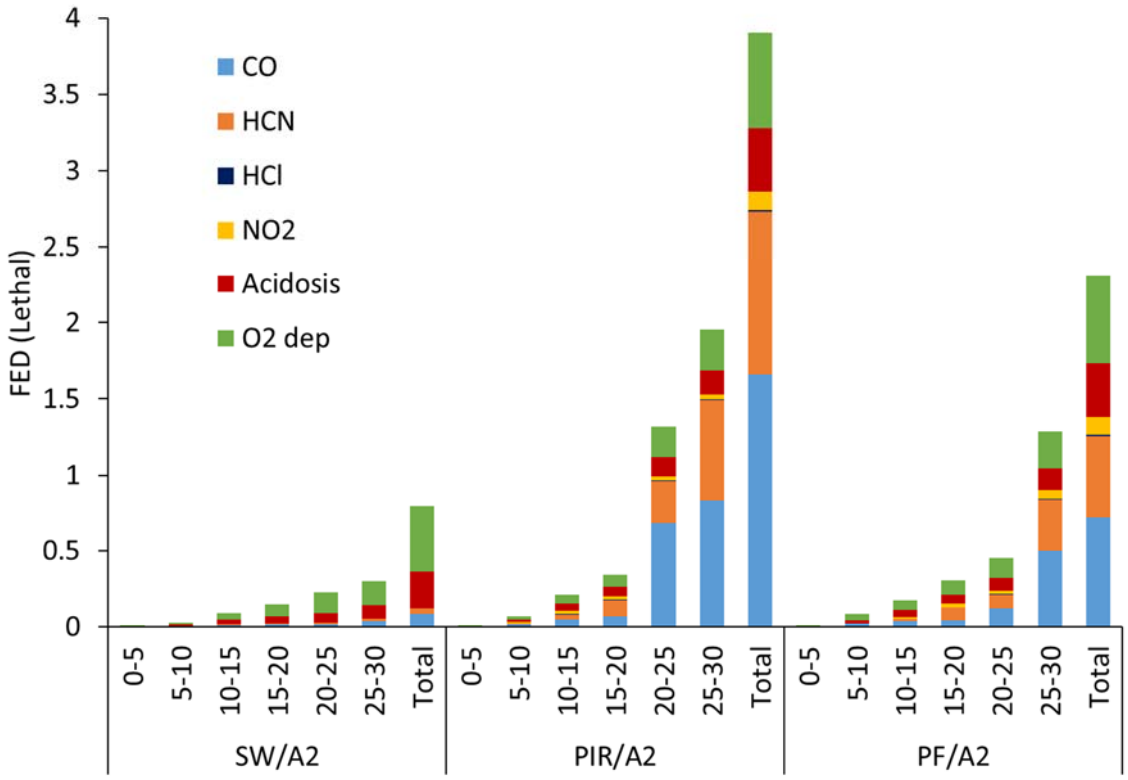

Figure 13 Individual toxicant contribution to total lethal FEDs at each 5 minute time period

Typically, in a high-rise building fire, with a combination of façade systems, the apartment above that of the fire origin may be exposed to a fairly well-ventilated cellulosic fire, while other apartments would predominantly be exposed to effluent derived from the burning façade. The chart appears to show the significant contribution that acidosis and oxygen depletion makes to the total FED. However, if a larger hypothetical room had been used for calculation the effects of acidosis and hypoxia would become insignificant. Acidosis and hypoxia are most significant for SW/A2 where they are the main contributors to the lethal FED, with a small contribution from CO, mostly from the burning wood crib and a small amount of HCN from the 5% binder in the stone wool.

For PIR/A2 and PF/A2, CO and HCN made a greater contribution to the FED, in addition to low O2 and acidosis. This resulted in the total FED being around 3.7 for PIR/A2 and 2.2 for PF/A2, compared to a value of 0.8 from the burning crib for the non-combustible system SW/A2.

4 Conclusions

The baseline results show that there is little difference in the toxicity of the smoke sampled at the main exhaust for different façade systems. Toxicity measured at the main exhaust is largely derived from the smoke toxicity of the wood crib with minimal contribution from the façade system.

At the main exhaust, the gases measured during all tests were characteristic of well-ventilated flaming combustion. Behind the cavity, the gases measured were characteristic of the well-ventilated combustion of the wood crib until the insulation started to burn. Once this occurred, we have shown that the combustion became under-ventilated, explaining why the concentrations of the toxic gases, CO and HCN increased markedly.

The addition of a vent into the façade system allowed the toxicity of the smoke within the cavity to be quantified. Although the flow in a real fire will depend on many factors, the enhanced toxicity close to where occupants may be trapped illustrates the hazard. Measuring toxicity in this way is a realistic way of assessing toxicity of smoke able to enter an apartment via a kitchen or bathroom vent, broken window or a void in the building's construction, from a façade fire. However, more precise prediction would require data on actual smoke flows from façades and cavities into real buildings under the full range of construction and weather conditions.

For PIR/A2, the toxicity of the smoke within the cavity was 40 times greater in terms of incapacitation and 5 times greater in terms of lethality than the smoke outside the façade. This is principally due to the increase in toxicity as a function of under-ventilation. In terms of the toxicity in the vent, a critical point occurred in both of the tests with ACM-A2 and combustible insulation, when the fire broke into the section of the cavity containing the vent, with the vast resultant increase in smoke toxicity.

To the best of our knowledge this is the first time the fire conditions have been quantified in rainscreen façade systems, and the first time the smoke toxicity within the cavity has been assessed.

PIR/PE produced a ferocious fire resulting in the early termination of the test at 13.5 min. At that time, the FEDs for both incapacitation and lethality had already started to increase much earlier than for any other material combination and would be expected to be significantly larger due to the size of the fire, had it been safe to continue the test.

The FED data show that concentrations of toxic gases would become incapacitating, then lethal for PIR/A2 fastest, followed by PF/A2 and then SW/A2.

The combination of under-ventilated flaming within the rainscreen façade, and combustible polymeric foam, has clear implications for fire safety. The increased smoke toxicity from the burning façade, through the nitrogen content of the foams and their use of gas phase flame retardants, would result in a very high toxic load in the event of a fire. The proximity of people's homes and living spaces to a facade with such toxic potential presents an unreasonably large hazard in the event of a developed fire in a neighbouring apartment.

5 Acknowledgements

This research did not receive any specific grant from funding agencies in the public, commercial, or not-for-profit sectors. We very gratefully acknowledge the RISCAuthority/Fire Protection Association for providing facilities and arranging construction of the test walls, Ash and Lacy Ltd for provision of ACM panelling and fixtures, and to Arup for providing designs and drawings of the test wall facades.

References

1. Babrauskas, V., *The Grenfell Tower Fire and Fire Safety Materials Testing* (2018) https://www.fireengineering.com/articles/print/volume-171/issue-1/features/the-grenfell-tower-fire-and-fire-safety-materials-testing.html (accessed 07/06/2020)
2. Choi, K.K., Taylor, W., *Combustibility of insulation in cavity walls*, (1984) Journal of Fire Sciences, 2 (3), pp. 179-188. https://www.doi.org/10.1177/073490418400200303
3. *Acceptability of common wall constructions containing combustible materials in high rise buildings,* NHBC Technical Services Building Regulations Technical Guidance Note – TS-EXTGN-BC-ADB-514v1-July 2016 (withdrawn July 2017). Referred to in section 5.2.86 of Colin

Todd's Expert report to the Grenfell Tower Inquiry https://assets.grenfelltowerinquiry.org.uk/documents/Colin%20Todd%20report_0.pdf (accessed 07/06/2020)

4. Colwell, S. and Baker, T. (2013), BR 135*: Fire Performance of external thermal insulation for walls of multistorey buildings*, BRE Trust, Watford.
5. Schulz, J., Kent, D., Crimi, T. et al. *A Critical Appraisal of the UK's Regulatory Regime for Combustible Façades*. Fire Technol (2020). https://doi.org/10.1007/s10694-020-00993-z
6. Professor Luke Bisby's expert report, Phase 1, Grenfell Tower Inquiry. https://www.grenfelltowerinquiry.org.uk/evidence/professor-luke-bisbys-expert-report (accessed 15/11/19)
7. UK Fire statistics 2020 and Preceding Editions, Home Office, London. https://www.gov.uk/government/collections/fire-statistics.
8. Stec, A.A., Hull, T.R., *Assessment of the fire toxicity of building insulation materials,* (2011) Energy and Buildings, 43 (2-3), pp. 498-506. https://www.doi.org/10.1016/j.enbuild.2010.10.015
9. McKenna, S.T., Hull, T.R. The fire toxicity of polyurethane foams. *Fire Sci Rev* **5,** 3 (2016). https://doi.org/10.1186/s40038-016-0012-3
10. Bengtström, L., Salden, M. & Stec, A.A. The role of isocyanates in fire toxicity. *Fire Sci Rev* **5,** 4 (2016). https://doi.org/10.1186/s40038-016-0013-2
11. Blomqvist, P., Hertzberg, T., Dalene, M., Skarping, G., *Isocyanates, aminoisocyanates and amines from fires - a screening of common materials found in buildings,* (2003) Fire and Materials, 27 (6), pp. 275-294. https://www.doi.org/10.1002/fam.836
12. D. Purser, 'Grenfell Tower Inquiry. Phase 1 - Expert report'. 2018. (accessed 7/6/2020) https://assets.grenfelltowerinquiry.org.uk/documents/Professor%20David%20Purser%20report%20%28Phase%201%20-%20supplemental%29%20DAPR0000001.pdf
13. New Civil Engineer. 1 July 1999. [Online]. Available: https://www.newcivilengineer.com/irvine-block-fire-sparks-overfacade-investigation/835807.article. (Accessed 13/2/19].
14. *Lakanal House Coroner Inquest*. Updated 7 April 2015. [Online]. Available: https://www.lambeth.gov.uk/elections-and-council/lakanal-house-coroner-inquest. [Accessed 6 February 2019].
15. BS 8414-1: 2015. *Fire Performance of External Facade Systems. Part 1: Test method for non-loadbearing external facade systems fixed to and supported by a masonry wall*. 2015. British Standards Institution.
16. GOV.UK. 11 August 2017. [Online]. Available: https://www.gov.uk/government/news/latest-government-large-scale-fire-safety-test-results-published.
17. GOV.UK. https://www.gov.uk/government/publications/fire-test-report-mhclg-bs-8414-hpl
18. Stec, A.A., Hull, T.R., Lebek, K., Purser, J.A., Purser, D.A., *The effect of temperature and ventilation condition on the toxic product yields from burning polymers,* (2008) Fire and Materials, 32 (1), pp. 49-60. https://www.doi.org/10.1002/fam.955
19. Li, Z., Huang, S., Shi, L., Li, Z., Liu, Q., Li, M., *Reducing the flammability of hydrophobic silica aerogels by doping with hydroxides,* (2019) Journal of Hazardous Materials, 373, pp. 536-546. https://www.doi.org/10.1016/j.jhazmat.2019.03.112
20. Woolley, W.D., Raftery, M.M., *Smoke and toxicity hazards of plastics in fires*, (1975) J. Hazard. Mater., 1 (3), pp. 215-222. https://doi.org/10.1016/0304-3894(75)80014-8
21. Mitchener, G., *Impact of Grenfell Tower fire disaster on polyisocyanurate industry,* (2018), Polimery/Polymers, 63 (10), pp. 716-722. https://www.doi.org/10.14314/polimery.2018.10.8
22. Molyneux, S., Stec, A.A., Hull, T.R., *The effect of gas phase flame retardants on fire effluent toxicity*, (2014) Polymer Degradation and Stability, 106, pp. 36-46. https://www.doi.org/10.1016/j.polymdegradstab.2013.09.013

23. European Chemicals Agency (ECHA) *Screening Report. An Assessment of Whether the Use of TCEP, TCPP, and TDCP in Articles Should Be Restricted*, (2018), https://echa.europa.eu/documents/10162/df7715f2-e413-8396-119b-63f929bcde0c
24. Lai, N.L.S., Kwok, K.Y., Wang, X.-H., Yamashita, N., Liu, G., Leung, K.M.Y., Lam, P.K.S., Lam, J.C.W. *Assessment of organophosphorus flame retardants and plasticizers in aquatic environments of China (Pearl River Delta, South China Sea, Yellow River Estuary) and Japan (Tokyo Bay),* (2019) Journal of Hazardous Materials, 371, pp. 288-294. https://www.doi.org/10.1016/j.jhazmat.2019.03.029
25. de la Torre, A., Navarro, I., Sanz, P., de los Ángeles Martínez, M., *Organophosphate compounds, polybrominated diphenyl ethers and novel brominated flame retardants in European indoor house dust: Use, evidence for replacements and assessment of human exposure,* (2020) Journal of Hazardous Materials, 382, art. no. 121009. https://www.doi.org/10.1016/j.jhazmat.2019.121009
26. Liu, X., Hao, J., Gaan, S., *Recent studies on the decomposition and strategies of smoke and toxicity suppression for polyurethane based materials*, (2016) RSC Advances, 6 (78), pp. 74742-74756. https://www.doi.org/10.1039/c6ra14345h
27. Cai, W., Cai, T., He, L., Chu, F., Mu, X., Han, L., Hu, Y., Wang, B., Hu, W., *Natural antioxidant functionalization for fabricating ambient-stable black phosphorus nanosheets toward enhancing flame retardancy and toxic gases suppression of polyurethane,* (2020) Journal of Hazardous Materials, 387, art. no. 121971. https://www.doi.org/10.1016/j.jhazmat.2019.121971
28. Wang, J., Zhang, D., Zhang, Y., Cai, W., Yao, C., Hu, Y., Hu, W., *Construction of multifunctional boron nitride nanosheet towards reducing toxic volatiles (CO and HCN) generation and fire hazard of thermoplastic polyurethane,* (2019) Journal of Hazardous Materials, 362, pp. 482-494. https://www.doi.org/10.1016/j.jhazmat.2018.09.009
29. Liu, X., Zhou, Y., Hao, J., Du, J., Smoke and toxicity suppression by zinc salts in flame-retardant polyurethane-polyisocyanurate foams filled with phosphonate and chlorinated phosphate, (2015) Journal of Applied Polymer Science, 132 (16), 41846. https://www.doi.org/10.1002/app.41846
30. McKenna, S.T., Jones, N., Peck, G., Dickens, K., Pawelec, W., Oradei, S., Harris, S., Stec, A.A., Hull, T.R., *Fire behaviour of modern façade materials – Understanding the Grenfell Tower fire,* (2019) Journal of Hazardous Materials, 368, pp. 115-123. https://www.doi.org/10.1016/j.jhazmat.2018.12.077
31. RISCAuthority Interim Project Report: *Occupant toxic exposure to fires in rain-screen cladding systems*. November 2018. https://www.thefpa.co.uk/news/news_detail.fpa-toxic-smoke-testing-results.html
32. Bonner, M., Rein, G., *Flammability and multi-objective performance of building façades: Towards optimum design,* (2018) International Journal of High-Rise Buildings, 7 (4), pp. 363-374. https://www.doi.org/10.21022/IJHRB.2018.7.4.363
33. Dr Barbara Lane 'Grenfell Tower Inquiry. Phase 1 - Expert report'. (2018). https://www.grenfelltowerinquiry.org.uk/evidence/dr-barbara-lanes-expert-report (accessed 7/6/2020)
34. ISO 13571:2012. 'Life-threatening components of fire - Guidelines for the estimation of time to compromised tenability in fires'. ISO, Geneva.
35. ISO 13344:2015. 'Estimation of the lethal toxic potency of fire effluents'. ISO, Geneva.
36. Statutory Guidance: *Approved Document B (fire safety) volume 1: Dwellings.* (2019), Ministry of Housing, Communities & Local Government, UK. https://www.gov.uk/government/publications/fire-safety-approved-document-b
37. ISO 19701: 2013. *Methods for Sampling and Analysis of Fire Effluents*. ISO, Geneva.

38. Hull, T.R., Carman, J.M., Purser, D.A., *Prediction of CO evolution from small-scale polymer fires,* (2000) Polymer International, 49 (10), pp. 1259-1265. https://www.doi.org/10.1002/1097-0126(200010)49:10<1259::AID-PI573>3.0.CO;2-D
39. Purser, D., Purser, J., *HCN yields and fate of fuel nitrogen for materials under different combustion conditions in the ISO 19700 tube furnace and large-scale fires,* (2008) Fire Safety Science, pp. 1117-1128. https://www.doi.org/10.3801/IAFSS.FSS.9-1117
40. ISO 19706: 2011. *Guidelines for assessing the fire threat to people*. ISO, Geneva.